

Fatigue Behaviour of DLC Coated Magnesium Alloy in Laboratory Air and Demineralized Water

Yoshihiko Uematsu^{1, a}, Keiro Tokaji^{1, b}, Hideaki Takekawa¹

¹Gifu University, 1-1 Yanagido, Gifu 501-1193, Japan

^ayuematsu@gifu-u.ac.jp, ^btokaji@gifu-u.ac.jp

Keywords: DLC, Fatigue, Corrosion fatigue, Magnesium alloy, Crack initiation

Abstract. Rotary bending fatigue tests were performed in laboratory air and demineralized water using DLC-coated wrought magnesium (Mg) alloy, AZ80. Two film thicknesses, 3.5 μ m and 25 μ m, were evaluated in order to investigate the effect of DLC coating on fatigue and corrosion fatigue behaviour. In laboratory air, the fatigue strengths of the DLC-coated specimens were higher than those of the bare ones and increased with increasing film thickness. This was because hard DLC film with high coating adhesion suppressed slip deformation on the specimen surface. In demineralized water, fatigue strengths were considerably decreased due to the formation of corrosion pits in the bare specimens. Thin DLC film could not improve corrosion fatigue strength due to the penetration of the solution through the pre-existed hole defects in the film, while thick DLC film could improve corrosion fatigue strength because penetrating paths were eliminated during long and two-step DLC deposition process of 26 hours.

Introduction

Magnesium (Mg) alloys are attractive as load-bearing components because of their superb properties, such as high strength/weight ratio, machinability and recyclability. Although they are increasingly used in the automotive and aeroplane industries, some shortcomings of them restrict the practical applications. The major shortcomings are low absolute strength and poor corrosion resistance compared with other light weight metals, such as Aluminium (Al) alloys. The protective hard coating on Mg alloy substrate is one of the effective ways to improve those properties. For example, anodic oxidation is the most popular method to make hard coating on Mg or Al alloys [1, 2]. However, anodising sometimes has the adverse effect on fatigue properties [1, 2], which are extremely important for structural components.

Recently, it is believed that diamond-like carbon (DLC) film could be the promising candidate for the coating which could improve both fatigue properties and corrosion resistance due to the high hardness, high coating adhesion, low defect density and chemical inertness. Some research works have been performed in order to investigate corrosion and friction wear properties using DLC coated Mg alloys [3-6], and preferable effects of DCL coating have been obtained. However, the effect of DCL coating on fatigue and corrosion fatigue properties of Mg alloys has not been understood. DLC films are deposited on the substrate using chemical vapour deposition (CVD), ion beam assisted deposition (IBAD) and so on. However, the practical coating thickness of DLC films deposited by those conventional methods is generally less than a few microns and it is difficult to deposit thicker films because of high internal stress of DLC film. The novel technique of a plasma enhanced chemical vapour deposition (PECVD) [7-9] could deposit much thicker films up to 70 μ m with relatively low internal stress. Furthermore, the temperature during PECVD process does not exceed 150°C, which is favourable to the coating on light weight metals. However, the effect of thick DLC coating on mechanical and fatigue properties has not been studied.

In this study, DLC film was deposited on extruded AZ80 by a PECVD method with two different thicknesses of 3.5 μ m and 25 μ m. Rotary bending fatigue tests have been performed in laboratory air

and demineralized water and the effect of DLC coating on fatigue and corrosion fatigue behaviour was discussed.

Experimental Details

Materials. The material used is extruded AZ80 alloy whose chemical compositions (wt.%) are listed in Table 1. Figure 1 shows the microstructure of the as-received material on the cross section perpendicular to the extrusion direction. The microstructure consists of equiaxed grains whose average size is $13\mu\text{m}$. Smooth fatigue specimens shown in Fig.2 with a diameter of 8mm and a gauge length of 10mm were machined from the extruded bars. Before DLC deposition, specimens were mechanically polished using progressively finer grades of emery paper and buff-finished.

Diamond-like Carbon Deposition. The DLC film was deposited on the gauge part of the specimen by means of a PECVD method, in which a high frequency plasma process using a mixture of hydrocarbons such as methane and inert gases such as argon at subatmospheric pressure was performed. The deposition was conducted under two conditions where the temperature was 150°C and the processing times were 3h and 26h. The different thicknesses of the film of $3.5\mu\text{m}$ and $25\mu\text{m}$ were achieved by short and long processing times, respectively. Furthermore, the thicker film was deposited by a two-step procedure, where the first step was terminated at 13h and then the second step was continued for 13h under the same condition. This two-step process was applied in order to reduce hole defects in the film aiming at higher corrosion resistance. In this study, a common silicon-based thin interlayer was not used between substrate and DLC film.

Procedures. Fatigue tests were performed using bare, $3.5\mu\text{m}$ and $25\mu\text{m}$ DLC-coated specimens by means of a 98Nm capacity rotary bending fatigue testing machine operating at a frequency of 20 Hz in laboratory air. Corrosion fatigue tests were conducted using the same testing machine where demineralized water was dropped onto the centre of gauge length by a metering pump whose flow rate was 140ml/min. It is well known that AZ series Mg alloy has aging ability [10] and the DLC deposition procedure at 150°C for 26h might affect the mechanical properties of test samples due to age hardening. Therefore, a part of bare specimens were T5 treated at 150°C for 26h and fatigue tests in air were conducted in order to identify the aging effect on fatigue behaviour.

Table 1 Chemical composition of material (wt.%).

	Al	Zn	Mn	Si	Cu	Fe	Ni	Mg
AZ80	8.3	0.6	0.3	0.03	0.003	0.002	<0.001	Bal.

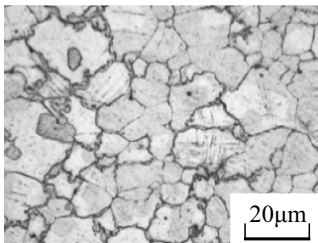


Fig. 1 Microstructure.

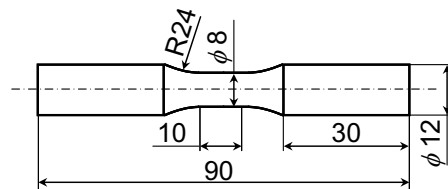


Fig. 2 Fatigue specimen configuration.

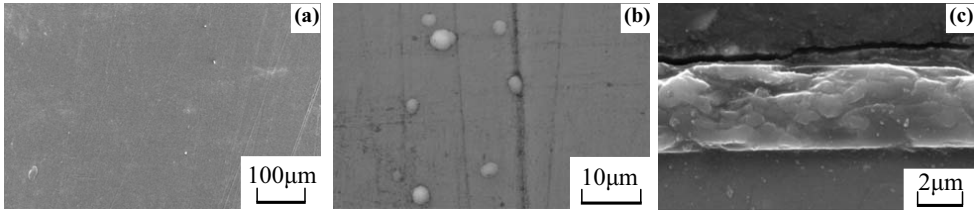


Fig. 3 Appearance of 3.5µm DLC film: (a) and (b) surface, (c) cross section.

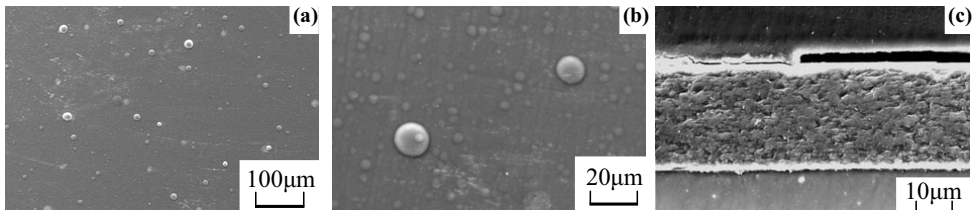


Fig. 4 Appearance of 25µm DLC film: (a) and (b) surface, (c) cross section.

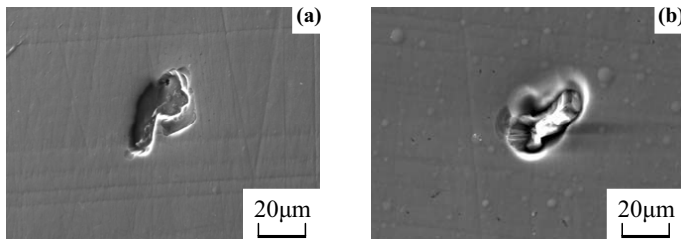


Fig. 5 Hole defects in the film: (a) 3.5µm DLC, (b) 25µm DLC.

Results

Coating Appearance. Figures 3 and 4 reveal the SEM micrographs showing the surface appearance and the cross section of 3.5µm and 25µm DLC films, respectively. Both surfaces were flat and smooth (Figs.3 (a) and 4(a)), but some spherical spots were observed in high magnification views (Figs.3 (b) and 4(b)). The number and size of spots are larger in 25µm DLC film. As shown in Figs.3 (c) and 4(c), DLC films are dense without any defects and crackings irrelevant to film thickness. The thickness of film was defined from these cross sectional images. The typical hole defects observed on the surface are shown in Figs.5 (a) and (b) for 3.5µm and 25µm DLC films, respectively. These defects are about 20µm, but the number of defects is very small.

Mechanical Properties. The mechanical properties of the bare, T5-treated and 25µm DLC-coated specimens are shown in Table 2. The effect of DLC film is not seen, while the tensile strength of the T5-treated specimen is slightly higher than that of the bare specimen.

Table 2 Mechanical properties of materials.

	0.2% proof stress $\sigma_{0.2}$ (MPa)	Tensile strength σ_B (MPa)	Elongation δ (%)	Elastic modulus E (GPa)
Bare	240	333	17.4	42
T5-treated	259	356	14.9	44
25 μ m DLC-coated	234	330	-	45

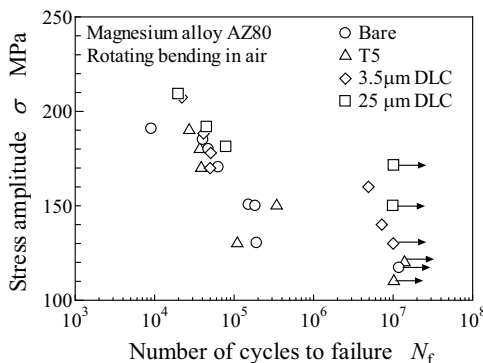


Fig. 6 *S-N* diagram in laboratory air.

Fatigue Behaviour in Laboratory Air.

Fatigue Strength. Figure 6 represents the *S-N* diagram for the bare, T5-treated, 3.5 μ m and 25 μ m DLC-coated specimens in laboratory air. The fatigue strength of the bare specimens is similar to that of the T5-treated ones, which have the same thermal history with the 25 μ m DLC deposition process. This indicates that the effect of the thermal history during DLC deposition on fatigue strength could be neglected. The DLC-coated specimens exhibit higher fatigue strength than the bare ones, and the fatigue strength is dependent on film thickness. The fatigue strengths at $N=10^7$ cycles are 120MPa, 130MPa and 170MPa for the bare, 3.5 μ m and 25 μ m DLC-coated specimens, respectively, indicating that the thicker film could achieve higher fatigue strength.

Crack Initiation. Figure 7 (a) shows the SEM micrograph of fracture surface near the crack initiation site of a bare specimen. A facet can be seen at the crack initiation site, indicating that cracks are generated due to cyclic slip deformation. The crack initiation site observed on the specimen surface is also shown in Fig.7 (b). As shown in the figure, inclusions are recognized near the crack initiation site. Those inclusions are considered to be Al-Mn-based intermetallic compound because the crack initiation from Al-Mn-based intermetallic compound has been reported in AZ series Mg alloys [11-13]. It reveals that the crack initiation in the bare specimen is due to slip deformation near the boundary of inclusion and the matrix. Figures 8 (a) and (b) represent the SEM micrographs of fracture surface near the crack initiation site of 3.5 μ m and 25 μ m DLC-coated specimens, respectively. In both figures, a facet can also be seen, indicating that crack initiation was due to cyclic slip deformation. It should be noted that the DLC film is still on the substrate around the crack initiation site in both specimens, indicating high coating adhesion regardless of film thickness.

Fatigue Behaviour in Demineralized Water.

Fatigue Strength. Figure 9 represents the *S-N* diagram for the bare, 3.5 μ m and 25 μ m DLC-coated specimens in demineralized water. The test results in laboratory air and demineralized water are shown by open and solid symbols, respectively. The effect of T5-treatment on fatigue strength was not seen in laboratory air. Hence, fatigue tests using the T5-treated specimen were not conducted in

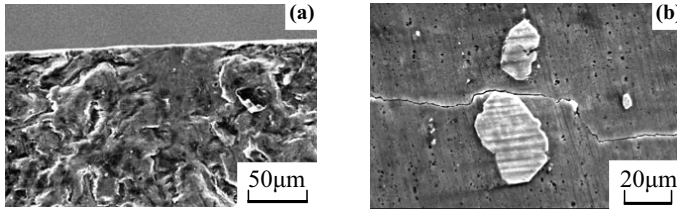


Fig. 7 SEM micrographs showing crack initiation site of bare specimen ($\sigma=150\text{MPa}$): (a) fracture surface, (b) specimen surface.

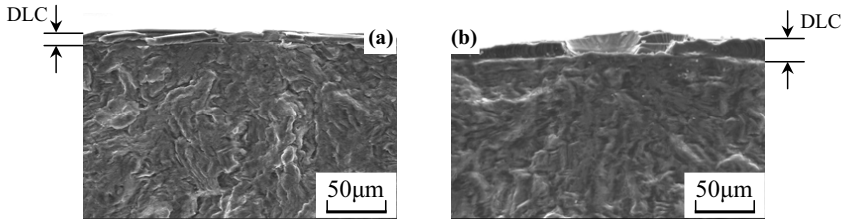


Fig. 8 SEM micrographs showing crack initiation site ($\sigma=180\text{MPa}$): (a) $3.5\mu\text{m}$ DLC, (b) $25\mu\text{m}$ DLC.

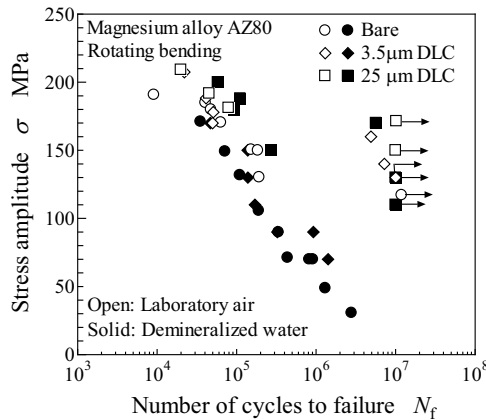


Fig. 9 $S-N$ diagram in demineralized water.

demineralized water. The fatigue strengths at high stress levels in demineralized water are similar to those in laboratory air in all specimens. In the bare and $3.5\mu\text{m}$ DLC-coated specimens, however, fatigue fracture occurs at stress levels much lower than the fatigue limit in laboratory air, and the fatigue limit is not seen in demineralized water. Furthermore, the $3.5\mu\text{m}$ DLC-coated specimen that had higher fatigue strength than the bare specimen in laboratory air exhibits nearly the same fatigue strength as the bare specimen in demineralized water. This indicates that thin DLC film could not improve corrosion fatigue strength. On the contrary, the fatigue strength of the $25\mu\text{m}$ DLC-coated specimen in demineralized water is much higher than those of the bare and $3.5\mu\text{m}$ DLC-coated specimens. The $25\mu\text{m}$ DLC-coated specimen shows clear fatigue limit, and the fatigue strength at $N=10^7$ cycles is 130MPa , which is lower than that in laboratory air, but higher than that of the bare specimen, indicating that the corrosion fatigue resistance was greatly improved by thick DLC film.

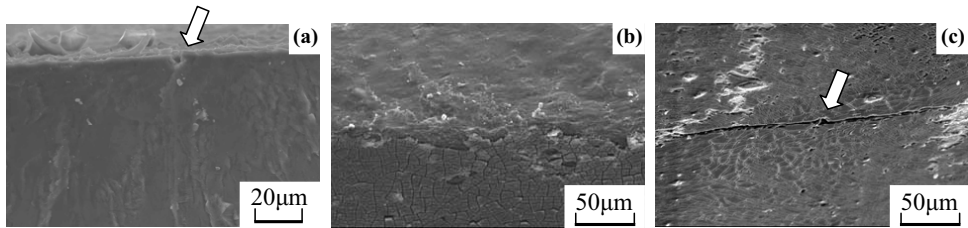


Fig. 10 SEM micrographs showing crack initiation site of bare specimen ($\sigma=70\text{MPa}$): (a) fracture surface, (b) tilted view, (c) non propagating crack.

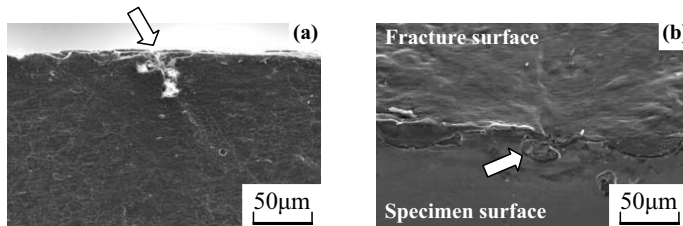


Fig. 11 SEM micrographs showing crack initiation site of 3.5 μm DLC-coated specimen: (a) fracture surface ($\sigma=90\text{MPa}$), (b) tilted view ($\sigma=130\text{MPa}$).

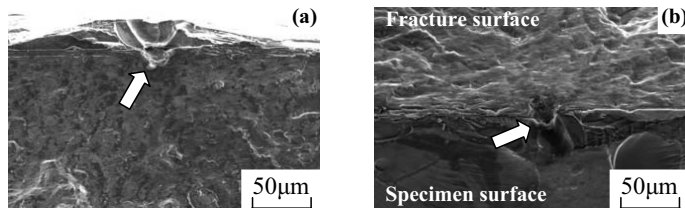


Fig. 12 SEM micrographs showing crack initiation site of 25 μm DLC-coated specimen ($\sigma=170\text{MPa}$): (a) fracture surface, (b) tilted view.

Crack Initiation. Figures 10-12 show the SEM micrographs of fracture surfaces near the crack initiation site of the bare, 3.5 μm and 25 μm DLC-coated specimens in demineralized water, respectively. In figure (b), the specimen was tilted about an angle of 45 degrees in order to observe the specimen surface. In the bare specimen (Figs.10 (a) and (b)), the specimen surface is covered by cracked corrosion product, and corrosion pit shown by arrow is recognized at the crack initiation site. Furthermore, a non-propagating crack initiated from corrosion pit was observed on the specimen surface as shown in Fig.10 (c). The crack initiation from corrosion pit in demineralized water has been reported in AZ and AM series Mg alloys [12]. In the 3.5 μm and 25 μm DLC-coated specimens (Figs.11 and 12), corrosion product is not seen on the specimen surface, while corrosion pit is observed at the crack initiation site similar to the bare specimen. DLC film remains on the surface near the crack initiation site, indicating the high coating adhesion.

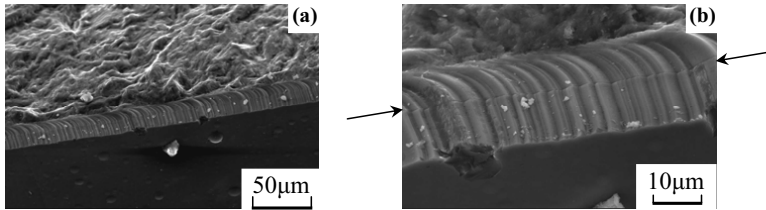


Fig. 13 Appearance of 25µm DLC film observed on crack growth path ($\sigma=240\text{MPa}$).

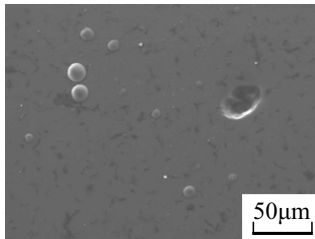


Fig. 14 Surface appearance of 25µm DLC-coated specimen after fatigue test in demineralized water ($\sigma=130\text{MPa}$, run out).

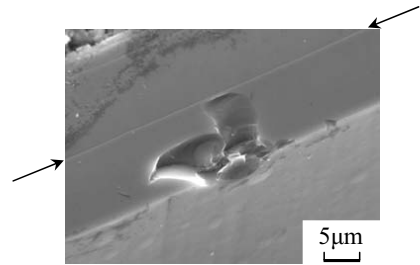


Fig. 15 Hole defect observed in 25µm DLC film ($\sigma=240\text{MPa}$).

Discussion

Fatigue Behaviour in Laboratory Air. As shown in Fig.6, the fatigue strengths of the DLC-coated specimens were higher than that of the bare one, and thicker film resulted in higher fatigue strength. Figure 13 shows the appearance of 25µm DLC film observed on the fatigue crack growth path ($\sigma=240\text{MPa}$). It is evident that fatigue crack grew stably through the film leaving a striation like pattern. Delamination of the film occurred neither at crack initiation site nor through crack growth path. This indicates high coating adhesion regardless of film thickness. In addition, the Vickers hardness of DLC film deposited by PECVD is estimated about 2200 [9]. Consequently, high hardness and adhesion of DLC film suppressed slip deformation on the specimen surface and led to the higher fatigue strength than the bare specimen. It is believed that the thicker film could suppress slip deformation more effectively. It should be noted that in Fig.13 (b), a clear line indicated by arrows is recognized at the mid thickness of the film due to the two-step deposition process.

Fatigue Behaviour in Demineralized Water. In demineralized water, 3.5µm DLC film was not effective for improving corrosion fatigue strength. Figure 14 shows the surface appearance of a 25µm DLC-coated specimen after the fatigue test conducted at the stress of fatigue limit in demineralized water. The corrosion of the film is not seen on the surface. Although the number of the pre-existed hole defects in the film shown in Fig.5 is very small, the solution penetrated through the hole to the substrate, which brought about the formation of corrosion pits at the early stage of fatigue life. On the contrary, Fig.15 indicates the hole defects observed on the cross section of 25µm DLC film. It reveals that the bottom of the hole reaches the mid thickness of the film, but does not penetrate to the substrate. Accordingly, the two-step deposition process resulted in both thick film and elimination of the penetrating hole defects, which led to the higher corrosion fatigue resistance. However, the corrosion pit was also observed at the crack initiation site of the 25µm DLC-coated specimen (Fig.12) and the fatigue strength was decreased in demineralized water. It is believed that the thick DLC film is effective for improving corrosion resistance, but the penetration of the solution might have occurred due to the fatigue damage of DLC film at the late stage of fatigue life.

Conclusions

Rotary bending fatigue tests were conducted in laboratory air and demineralized water using bare, 3.5 μ m and 25 μ m DLC-coated AZ80. Fatigue strength was evaluated and the effect of DLC coating on fatigue fracture mechanisms was discussed based on experimental observation. The following conclusions can be made.

1. Both DLC-coated specimens exhibited higher fatigue strength than the bare specimen in laboratory, where thicker DLC film resulted in higher fatigue strength.
2. The fatigue strengths at $N=10^7$ cycles were 120MPa, 130MPa and 170MPa for the bare, 3.5 μ m and 25 μ m DLC-coated specimens, respectively.
3. In demineralized water, fatigue fracture occurred even if stress levels were much lower than the fatigue limit in laboratory air in the bare and 3.5 μ m DLC-coated specimens, while the fatigue strength of the 25 μ m DLC-coated specimen was much higher than those of the bare and 3.5 μ m DLC-coated specimens.
4. The fatigue strengths at $N=10^7$ cycles was 130MPa for the 25 μ m DLC-coated specimen, and no fatigue limit was observed for the other specimens in demineralized water.
5. In demineralized water, corrosion pits were observed at the crack initiation site in 3.5 μ m and 25 μ m DLC-coated specimens, indicating that the penetration of the solution occurred through the DLC film.

References

- [1] A.J. Eifert, J.P. Thomas and R.G. Rateick Jr.: Scripta Materialia Vol. 40 (1999), p. 929
- [2] A.L. Yerokhin, A. Shatrov, V. Samsonov, P. Shashkov, A. Leyland and A. Matthews: Surface & Coating Technology Vol. 182 (2004), p. 78
- [3] N. Yamauchi, K. Demizu, N. Ueda, N.K. Cuong, T. Sone and Y. Hirose: Surface & Coating Technology Vol. 193 (2005), p. 277
- [4] J. Choi, J. Kim, S. Nakao, M. Ikeyama and T. Kato: Nuc. Inst. and Methods Physics Research B Vol. 257 (2007), p. 718
- [5] J. Choi, S. Nakao, J. Kim, M. Ikeyama and T. Kato: Diamond and Related Materials Vol. 16 (2007), p.1361
- [6] N. Yamauchi, N. Ueda, A. Okamoto, T. Sone, M. Tsujikawa and S. Oki: Surface & Coating Technology Vol. 201 (2007), p. 4913
- [7] A. Dorner-Reisel, C. Schürer, G. Irmer and E. Müller: Surface & Coating Technology Vols. 177-178 (2004), p. 830
- [8] V.S. Sundaram: Surface & Coating Technology Vol. 201 (2006), p. 2707
- [9] D. Lusk, M. Gore, W. Boardman, T. Casserly, K. Boinapally, M. Oppus, D. Upadhyaya, A. Tudhope, M. Gupta, Y. Cao and S. Lapp: Diamond and Related Materials, in press
- [10] A.F. Crawley and K.S. Milliken: Acta Metallurgica Vol. 22 (1974), p. 557
- [11] Y. Uematsu, K. Tokaji, M. Kamakura, K. Uchida, H. Shibata and N. Bekku: Mater. Sci. Eng. A Vol. 437 (2006), p. 131
- [12] Y. Uematsu, K. Tokaji and T. Ohashi: Strength of Materials Vol. 40 (2008), pp.141
- [13] Z.B. Sajuri, Y. Miyashita, Y. Hosokai and Y. Mutoh: Int. J. Mech. Sci. Vol. 48 (2006), p. 198